Am J Cancer Res 2025;15(12):5281-5292
www.ajcr.us /ISSN:2156-6976/ajcr0167139

Original Article

USP5-mediated stabilization of ILF2 via deubiquitination drives the tumor growth of colorectal cancer

Wendao You[1,2*], Xin Xu[2*], Jun Ye[3*], Ximao Cui[4*], Kunkun Han[2], Guodong Chen[5], Peng Yang[6], Yili Yang[2,7]

[1]Department of Gastroenterology, The First Affiliated Hospital of Soochow University, Suzhou 215006, Jiangsu, P. R. China; [2]China Regional Research Center, International Centre for Genetic Engineering and Biotechnology, Taizhou 225300, Jiangsu, P. R. China; [3]The Center for Translational Medicine, The Affiliated Taizhou People's Hospital of Nanjing Medical University, Taizhou 225300, Jiangsu, P. R. China; [4]Department of Gastrointestinal Surgery, Shanghai East Hospital (East Hospital Affiliated to Tongji University), Shanghai 200092, P. R. China; [5]School of Basic Medical Sciences, Wannan Medical College, Wuhu 241002, Anhui, P. R. China; [6]Department of Emergency Medicine, The First Affiliated Hospital of Soochow University, Suzhou 215006, Jiangsu, P. R. China; [7]Translational Cancer Research Laboratory, Suzhou Acumen Medical Technology, Suzhou 215123, Jiangsu, P. R. China. [*]Equal contributors.

Received July 1, 2025; Accepted December 17, 2025; Epub December 25, 2025; Published December 30, 2025

Abstract: Interleukin enhancer binding factor 2 (ILF2) has been confirmed to drive the progression and proliferation of multiple malignancies, but the expression and function of ILF2 in colorectal cancer (CRC) remain to be elucidated. In this study, the expression of ILF2 in CRC tissues was evaluated by the public tumor databases, quantitative reverse transcription PCR (qRT-PCR) and tissue array analyses. ILF2 was found to be elevated in CRC, and was predicted to serve as a negative index for patients. Subsequently, cell proliferation was detected by Cell Counting Kit-8 (CCK-8) assay and colony formation, and tumor growth was evaluated by establishing xenografted mouse models. Our results showed that knockout of ILF2 markedly inhibited cell proliferation and tumor growth of CRC. Moreover, we found ILF2 was ubiquitinated, and further co-immunoprecipitation (Co-IP) coupled with liquid chromatography-tandem mass spectrometry analysis indicated that ILF2 may be a novel substrate of the deubiquitinating enzyme ubiquitin specific peptidase 5 (USP5). Further reciprocal Co-IP assays confirmed that ILF2 interacted with USP5. Enforced expression of USP5 reduced ubiquitinated ILF2 and increased ILF2 level, whereas catalytic inactive USP5 did not. While USP5 inhibitor WP1130 downregulated ILF2 and inhibited CRC cell growth, the effects were markedly abolished by ILF2 overexpression. These data demonstrate that the USP5/ILF2 axis mediates the tumorigenesis of CRC, which highlights the USP5/ILF2 axis as a promising therapeutic target for CRC treatment.

Keywords: Ubiquitin specific peptidase 5, interleukin enhancer binding factor 2, colorectal cancer, deubiquitination, cell growth

Introduction

Colorectal cancer (CRC) is one of the most aggressive tumors, and belongs to the third most common malignant tumor in the world with over 1.9 million new cases worldwide in 2020 [1-3]. Through studies carried out in the past decades, the impacts of many environmental factors on the development of CRC have been well identified by the researchers, such as diet, the gut microbiota and their metabolites [4]. However, people still cannot overcome these factors, and the global burden of CRC is continuously increasing [5]. Despite significant progress has been done in drug targeted therapy and immunotherapy for CRC in recent years, less than one-third of CRC patients have successfully benefited from targeted therapy and immunotherapy due to the presence of gene mutations in the body [6]. Finding new drug targets for the prevention and treatment of CRC remains very important.

Interleukin enhancer binding factor 2 (ILF2), also namely nuclear factor 45 (NF45), has been demonstrated to play important roles in regulating RNA stability, cell growth and inflammatory responses [7]. Recent studies have reported

https://doi.org/10.62347/FSPT8923

that ILF2 is involved in the tumorigenesis of several cancers by promoting cancer cell growth. For example, ILF2 was reported to be up-regulated in non-small cell lung cancer (NSCLC), and its high expression indicated a poor prognosis for NSCLC patients [8]. Moreover, silence of ILF2 inhibited NSCLC cell proliferation and cell cycle progression, which further suggested that ILF2 was involved in the pathogenesis of NSCLC [8]. In hepatocellular carcinoma (HCC), both of the mRNA and protein levels of ILF2 were highly expressed in tumor tissues, and upregulated ILF2 was proved to induce cell growth of HCC through in vitro and in vivo experiments [9]. ILF2 has also been reported to promote tumor cell growth or proliferation in small cell lung cancer [10], metastatic melanoma [11], pancreatic ductal adenocarcinoma [12] and esophageal squamous cell carcinoma [13]. However, little is known about ILF2 function in CRC.

The stability of protein is mainly regulated by the ubiquitin-proteasome system (UPS) and the lysosomal pathway, and the UPS is controlled through the cascade-dependent enzymatic reactions, including the ubiquitin-activating enzyme, ubiquitin-conjugating enzymes, ubiquitin ligases, and deubiquitinating enzymes (DUBs) [14, 15]. Among the DUBs, ubiquitin specific peptidase 5 (USP5) is a member of the ubiquitin-specific protease (USP) family [16]. Increasing evidences indicate that USP5 is involved in many cellular processes, including DNA repair, cell proliferation, stress reactions, and inflammatory responses [16]. It has been also shown that USP5 is upregulated in some human cancers, and our previous study also revealed that USP5 was elevated in CRC and facilitated CRC cell growth [17]. Moreover, several downstream target proteins of USP5 have been reported by several researchers, including FoxM1, β-catenin, PD-L1 and TUFM [16]. In this study, we confirmed that ILF2 was elevated in CRC tumor tissues, and its upregulation predicted a poor prognosis for CRC patients. Further in vitro and in vivo experiments revealed that ILF2 promoted CRC cell growth. The protein stability of ILF2 was also found to be enhanced by USP5. Inhibiting USP5 by WP1130 decreased the protein levels of ILF2 in CRC cells, and overexpression of ILF2 abolished the effects of WP1130 on cell viability of CRC.

Methods

Cells, tissues and chemicals

HCT116, HT29, LOVO, RKO, SW480, SW620 and SW948 cell lines were purchased from ATCC, Manassas, VA. HEK293T cell line was maintained in our laboratory. All the cells were cultured in Dulbecco's Modified Eagle Medium (Hyclone, Utah, USA) with 10% fetal bovine serum (BioChannel Biological Technology Co., Ltd., Nanjing, China), 100 U/ml penicillin and 100 μg/ml streptomycin (Beyotime, Beijing, China). The CRC paracancerous and cancerous specimens were collected from the Department of Colorectal Surgery, Xinhua Hospital, Shanghai JiaoTong University School of Medicine, Shanghai, China. The case information was reported by our previous study [17]. Informed consent was obtained from all the collections. The research protocol of this study was approved by the Institutional Ethics Committee of China Regional Research Center of International Centre for Genetic Engineering and Biotechnology (ICGEB20220107-1). MG1-32, puromycin, cycloheximide and WP1130 were purchased from Selleck Chemicals, Houston, Texas, USA.

Bioinformatics analyses

The public tumor database GEPIA matched TCGA normal and GTEx data was used to evaluate the expression of ILF2 in colon adenocarcinoma (COAD) and rectum adenocarcinoma (READ) online (http://gepia2.cancer-pku.cn), and default options were selected. Correlation analyses between ILF2 and MKI67, C-MYC, CCNB1, CCND1, CCNE1 or XIAP in COAD were also analyzed by GEPIA online (http://gepia2.cancer-pku.cn/#correlation). The degrons of human ILF2 protein were predicted by the online tool Degpred (http://degron.phasep.pro/detail/Q12905/) as described previously [18].

Quantitative reverse transcription PCR (qRT-PCR)

To evaluate the mRNA levels of ILF2 in CRC tissues, qRT-PCR analysis was performed as reported previously [19]. Briefly, total RNA was extracted with RNAiso Plus (Takara Bio Group, Japan), and then RNA was reversely transcribed into cDNA with PrimeScript™ RT reagent Kit (Takara Bio Group, Japan). SYBR Green qPCR

Master Mix (Takara Bio Group, Japan) was used for qRT-PCR analysis. Primers used in this study were as follows: ILF2, forward, 5'-CACACCCTGGATCCTTGACC-3', reverse, 5'-ACAGTCCTGCAGCCAGAATC-3'; GAPDH, forward, 5'-GCACCGTCAAGGCTGAGAAC-3', reverse, 5'-TGGTGAAGACGCCAGTGGA-3'.

Immunohistochemistry (IHC) analysis

The tissue arrays with 169 CRC Paracancerous and cancerous tissues were prepared for IHC analysis as described previously [17]. The primary anti-ILF2 antibody used for IHC analysis was purchased from ThermoFisher Scientific, USA, and the staining of ILF2 in the tissues was scored based on a semi-quantitative score: 0, negative; 1, weak; 2, moderate; 3, strong.

Generation of ILF2-knockout (ILF2-KO) or USP5-knockdown cells

To generate ILF2-KO HCT116 cells, single-guide RNA (sgRNA) sequence targeting ILF2 was selected, synthesized and cloned into the lenti-CRISPR V2 vector (Addgene_52961) as reported previously [20]. The lentivirus-delivered shRNAs against USP5 (shUSP5) were constructed as described previously [17]. To generate lentivirus, the indicated sgRNA plasmids or shRNAs along with packaging plasmids were co-transfected into HEK293T cells. Three days later, viral particles were harvested from the cell culture supernatant through ultracentrifugation method. The target sequences of shUSP5 were as follows: shUSP5#1, 5'-CTTTGCCTTCATTAGTCACAT-3'; shUSP5#2, 5'-GACCACACGATTTGCCTCATT-3'.

Immunoblotting (IB) analysis

Cells or tissues were lysed for IB analysis as previously reported [21]. Total protein was extracted by using RIPA lysis buffer (Beyotime, Beijing, China), and quantified by using Enhanced BCA Protein Assay Kit (Beyotime, Beijing, China). Thirty micrograms of total protein were subjected to SDS-PAGE, followed by evaluation with specific primary antibodies. The primary antibody against ILF2 was purchased from ThermoFisher Scientific, USA. The anti-CCND1 antibody was obtained from Cell Signaling Technology, Danvers, MA. Anti-GAPDH and anti-USP5 antibodies were bought from Proteintech Group, Wuhan, China. Primary antibodies against Flag tag and Myc tag were purchased from Medical & Biological Laboratories, Tokyo, Japan. The anti-Ub antibody was obtained from Santa Cruz Biotechnology, Santa Cruz, CA. The secondary antibodies HRP-labeled Donkey Anti-Goat IgG (H+L), HRP-labeled Goat Anti-Rabbit IgG (H+L) and HRP-labeled Goat Anti-Mouse IgG (H+L) were purchased from Beyotime, Beijing, China. The images of IB were visualized by using an ECL-chemiluminescence detection system (Bio-Rad, California, USA).

Cell growth, viability and colony formation analyses

To evaluate cell growth, indicated cells were cultured at different time points, and viable cells were measured at indicated time points by Cell Counting Kit-8 (CCK-8) assay (Selleck Chemicals, Houston, Texas, USA) as described previously [22]. To evaluate cell viability, cells were incubated with indicated chemicals for indicated time, followed by CCK-8 assay. To assess colony formation, cells were put in 6-well plates for 10 days, and then cells were fixed and stained with crystal violet (Beyotime, China). The colonies were counted and colony formation rate was calculated.

Xenograft models

Female nude mice (Shanghai SLAC Laboratory Animal, Shanghai, China) aged six to eight weeks were prepared for constructing xenograft tumor models. The nude mice were kept in a specific pathogen-free (SPF) environment under standard conditions. HCT116 cells with wild-type ILF2 (Ctr) or ILF2-KO were injected into the right flanks of the mice respectively (n = 5 mice per group). To minimize potential post-injection pain, analgesic management was administered as needed based on daily monitoring of animal behavior and clinical signs. One week later, the volumes of the tumors were measured every three days for continuously two weeks. At the end of the animal study, the animals were euthanized by CO_2 inhalation, followed by tumor extraction and weighing. All animal procedures were approved by the Institutional Animal Care and Use Committee of China Regional Research Center of International Centre for Genetic Engineering and Biotechnology, and conducted in accordance with its ethical guidelines.

Plasmids construction and transfection

The human full-length ILF2, USP5 or Ub CDS sequences were amplified by PCR, and subcloned into pcDNA3.1 vector with a Flag or Myc tag. And the catalytically inactive mutant of USP5 (C335A) was generated as described previously [17]. Plasmids were then transfected into CRC or HEK293T cells with Lipofectamine® 2000 (Invitrogen) according to the manufacturer's protocol.

Co-immunoprecipitation (Co-IP) assay

Co-IP was performed to evaluate the protein interactions as reported previously [23]. In brief, indicated cells were lysed with Pierce™ IP Lysis Buffer (ThermoFisher Scientific), and whole cell lysates were incubated with indicated primary antibodies overnight at 4°C. The mixture continued to be incubated with Protein A/G PLUS-Agarose (Santa Cruz Biotechnology) for 2 hours at 4°C, and then these agarose was washed, denatured and analyzed by IB.

Cycloheximide (CHX) chase assay

CHX chase assay was conducted as reported previously [24]. In brief, Myc-USP5 or Flag-ILF2 plasmids were transfected into HEK293T cells for 24 hours, and then transfected cells were incubated with 50 μg/ml CHX for indicated times. Cells were collected at different time points, and then lysed for IB analysis.

Statistical analysis

All the pictures generated in this paper were drawn by GraphPad Prism 8.0.2. Data were presented as mean ± SD. Student's *t* test was used to compare the differences between two groups. One-way ANOVA or two-way ANOVA was used to compare differences among three or more groups. $P < 0.05$ was considered statistically significant. The Kaplan-Meier method and Log-rank test were used to analyze the overall survival of CRC patients with low or high expression of ILF2.

Results

ILF2 is elevated in colorectal cancer and induces cancer cell proliferation

To evaluate the expression level of ILF2 in CRC, the public tumor databases were firstly used. As shown in **Figure 1A**, the database showed that ILF2 was significantly upregulated in both of the cancerous tissues from colon adenocarcinoma (COAD) and rectum adenocarcinoma (READ). Oncomine database also indicated the upregulation of ILF2 in colon adenocarcinoma (Supplementary Figure 1A). The primary CRC tissue samples also verified the upregulation of ILF2 in CRC tumor tissues by the qRT-PCR analysis (**Figure 1B**). Meanwhile, the tissue arrays detected by IHC analysis further showed that ILF2 was elevated in CRC tumor tissues (**Figure 1C** and **1D**). Kaplan-Meier survival curves based on IHC results and the public database Kaplan-Meier Plotter also showed that CRC patients with ILF2-high expression had a shorter overall survival than patients with low expression (**Figure 1E** and Supplementary Figure 1B), which indicated that elevated ILF2 was a negative index for CRC patients.

Further results of correlation analyses showed that ILF2 expression in COAD was positively correlated with the expression of growth-promoting genes, including MKI67, C-MYC, CCNB1, CCND1, CCNE1 and XIAP (Supplementary Figure 2). To better understand the function of ILF2 in CRC cells, ILF2 was knocked out by CRISPR/Cas9 technology (**Figure 1F**). Notably, the expression level of CCND1, a master regulator of the cell cycle in the G1 to S phase transition, was dramatically downregulated when ILF2 was knocked out (**Figure 1F**). We also found that knockout of ILF2 could significantly inhibit the cell proliferation of CRC (**Figure 1G** and **1H**). Then, cell-derived xenograft models were established, and we confirmed that knockout of ILF2 significantly suppressed the tumor growth of CRC, expressed by the tumor volume, tumor weight and CCND1 expression (**Figure 1I-K**). In contrast, overexpression of ILF2 significantly promoted the cell growth in both of HCT116 and SW480 cells (Supplementary Figure 3). Collectively, above information revealed that ILF2 promoted CRC cell proliferation, at least in part, by upregulating CCND1 to facilitate cell cycle progression.

ILF2 is ubiquitinated and regulated by the ubiquitin-proteasome pathway

Subsequently, we found that there were predicted degrons in the sequence of human ILF2 protein (**Figure 2A** and Supplementary Figure 4), which indicated that ILF2 may be regulated by the ubiquitin-proteasome system. To further

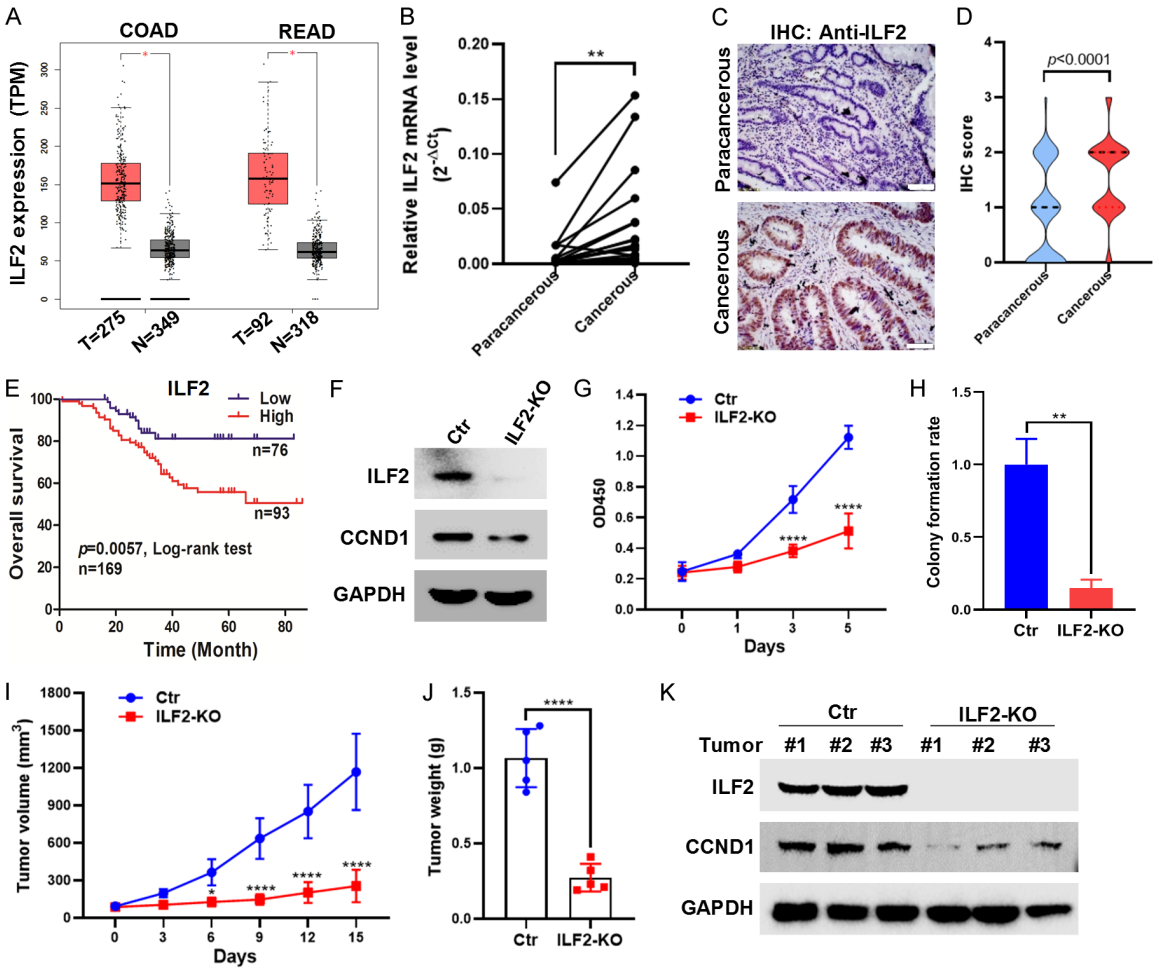

Figure 1. ILF2 is elevated in colorectal cancer and induces cancer cell growth. (A) The expression of ILF2 in colon adenocarcinoma (COAD) and rectum adenocarcinoma (READ) was predicted by GEPIA database online (http://gepia2.cancer-pku.cn). (B) Twenty pairs of paracancerous and cancerous tissues of colorectal cancer (CRC) were prepared for quantitative reverse transcription PCR (qRT-PCR) to analyze the mRNA levels of ILF2. GAPDH was used as an internal control. Data were analyzed by Student's *t* test. (C, D) The tissue arrays containing 169 CRC paracancerous and cancerous specimens were prepared for immunohistochemistry (IHC) analysis. Representative images (400×) and quantification of ILF2 IHC staining were as shown indicated (C, D). Data were analyzed by Student's *t* test. (E) Overall survival of CRC patients with low or high expression of ILF2 was analyzed by Kaplan-Meier survival curves. (F-H) ILF2 was knocked out in HCT116 cells, and ILF2-knockout (ILF2-KO) cells were generated, followed by immunoblotting (IB) analysis against ILF2, CCND1 and GAPDH (F). Cell proliferation was evaluated by Cell Counting Kit-8 (CCK-8) assay (G) and colony formation assay (H) as indicated. Data were the mean ± SD of three independent experiments. Data in (G) were analyzed by repeated measures two-way ANOVA followed by Bonferroni's post hoc test. Data in (H) were analyzed by Student's *t* test. (I) HCT116 cells with ILF2 knockout (ILF2-KO) or wild-type ILF2 (Ctr) were subcutaneously injected into the right flanks of nude mice. When tumors were palpable, tumor volumes were monitored every three days for continuously two weeks. n = 5 mice per group. Data were the mean ± SD, and analyzed by repeated measures two-way ANOVA followed by Bonferroni's post hoc test. (J, K) The tumors were also weighed (J), and prepared for IB analysis against ILF2, CCND1 and GAPDH (K). Data in (J) were the mean ± SD, and analyzed by Student's *t* test. $^{*}P < 0.05$, $^{**}P < 0.01$, $^{****}P < 0.0001$.

verify our hypothesis, the proteasome inhibitor MG132 was used, and our results showed that both of the exogenous ILF2 protein (**Figure 2B** and **2C**) and endogenous ILF2 protein (**Figure 2D** and **2E**) were upregulated after the treatment of MG132. Meanwhile, the Co-IP assay also revealed that ILF2 was poly-ubiquitinated and its poly-ubiquitination could be enhanced by the treatment of MG132 (**Figure 2F**). Taken together, these results indicated that ILF2 protein was regulated by the ubiquitin-proteasome system.

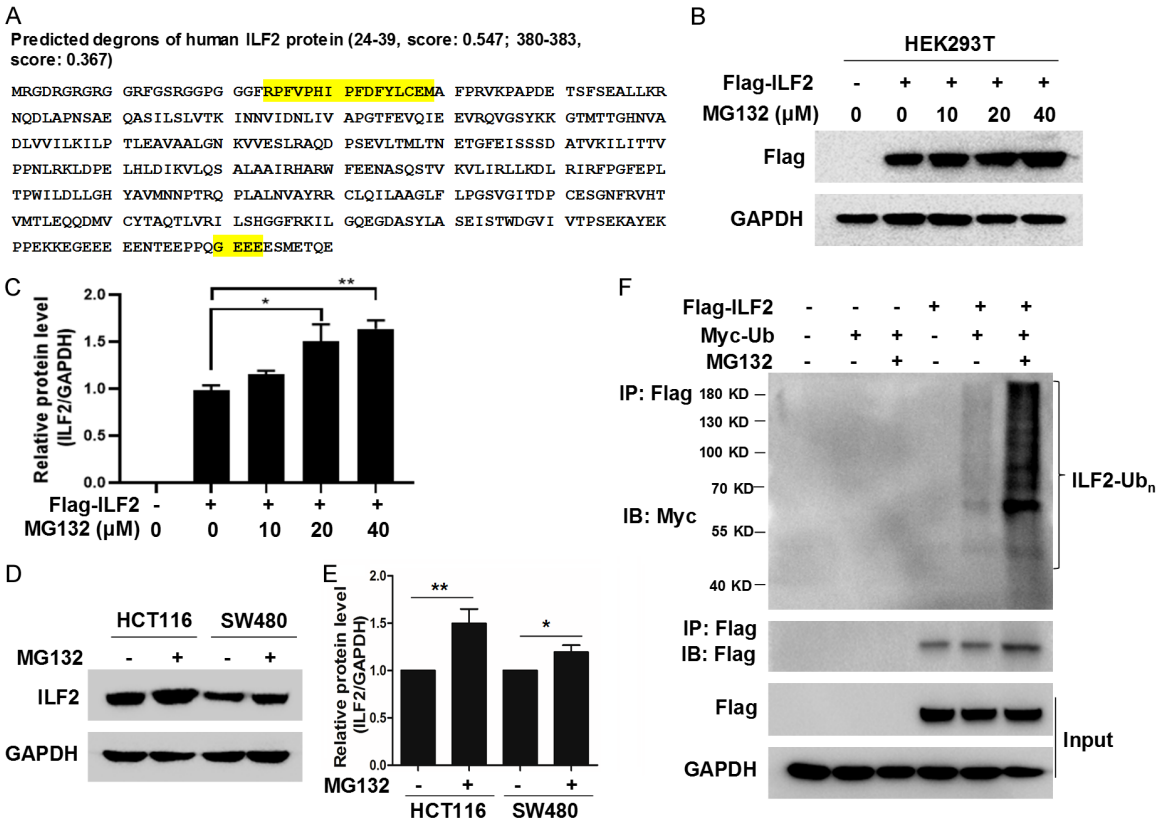

Figure 2. ILF2 is ubiquitinated and degraded by the proteasome. (A) Predicted degrons of human ILF2 protein (http://degron.phasep.pro/detail/Q12905/), and they were highlighted in yellow. (B, C) HEK293T cells were transfected with Flag-ILF2 plasmids for 24 hours, and then transfected cells were incubated with indicated MG132 for 6 hours, followed by immunoblotting (IB) against Flag and GAPDH (B). The optical density was also measured (C). (D, E) HCT116 and SW480 cells were treated with 20 μM MG132 for 6 hours, followed by IB against ILF2 and GAPDH (D). The optical density was also measured (E). (F) HEK293T cells were transfected with indicated Flag-ILF2 and Myc-Ub plasmids for 24 hours, and then transfected cells were incubated with 20 μM MG132 for 6 hours, followed by immunoprecipitation (IP) with an anti-Flag antibody. $^{*}P < 0.05$; $^{**}P < 0.01$.

Identification of ILF2 as a novel substrate of USP5

Interestingly, our previous liquid chromatography-tandem mass spectrometry (LC-MS/MS) analysis identified several interacting proteins of USP5, including ILF2 (**Figure 3A** and **3B**). To further confirm the protein interaction between ILF2 and USP5, reciprocal Co-IPs were carried out, and Co-IPs indicated that exogenous or endogenous ILF2 could bind to exogenous or endogenous USP5 (**Figure 3C** and **3D**). In addition, several CRC cell lines and primary tumor tissues were collected and prepared for immunoblotting analysis to detect the expression levels of ILF2 and USP5, and further correlation analysis showed that USP5 expression was positively correlated with ILF2 expression (**Figure 3E-G**), which further indicated that there was a certain connection between USP5 and ILF2.

USP5 accumulates ILF2 by reducing its polyubiquitination

As stated above that USP5 bound to ILF2, we next evaluated whether the protein level of ILF2 was regulated by USP5. As shown in **Figure 4A** and **4B**, overexpression of USP5 markedly increased both of the exogenous and endogenous protein levels of ILF2. However, the catalytically inactive mutant of USP5 lost its up-regulatory effect (**Figure 4B**). In contrast, knockdown of USP5 decreased the protein level of ILF2 in CRC cells (**Figure 4C**). Consistently, CHX chase assay also showed that overexpression of USP5 significantly prolonged the half-life of ILF2 protein (**Figure 4D** and **4E**). As known that

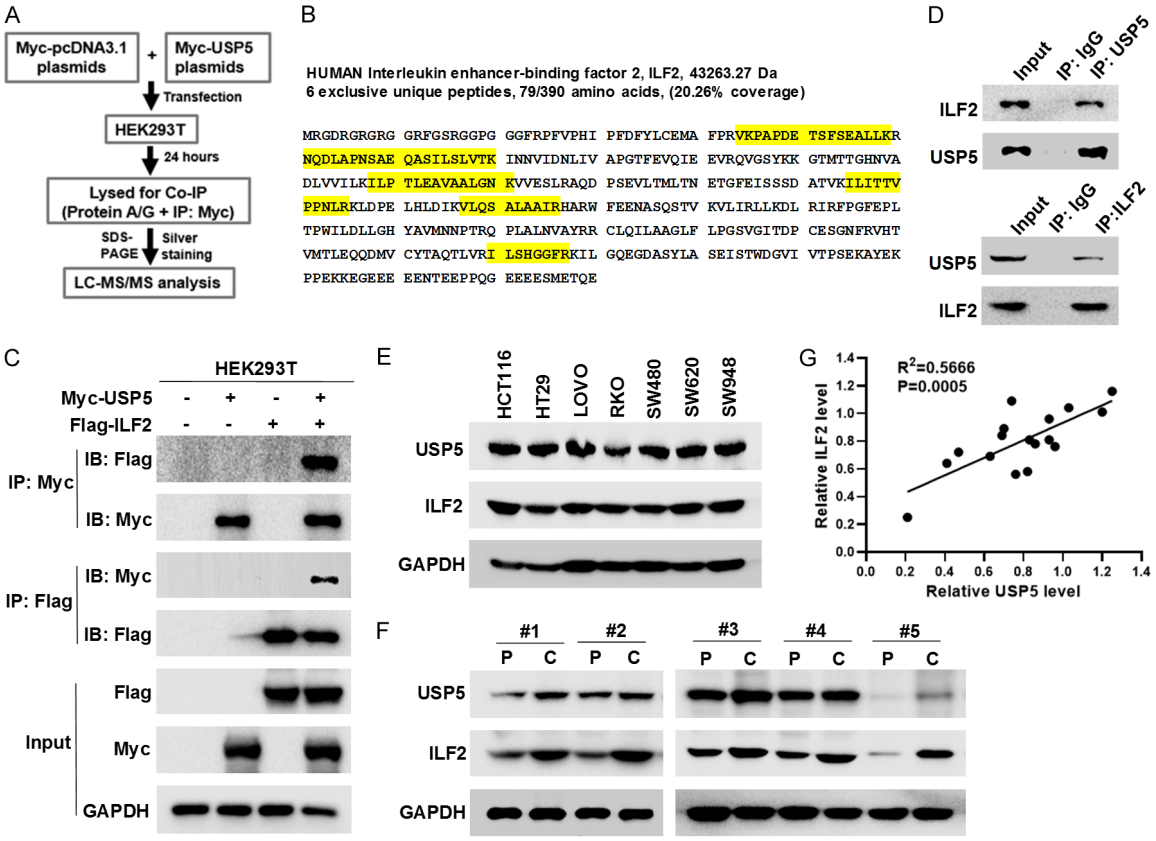

Figure 3. Identification of ILF2 as a novel substrate of USP5. (A) The flow chart of identifying interacting proteins of USP5. (B) Six exclusive unique peptides of ILF2 protein were identified by liquid chromatography-tandem mass spectrometry (LC-MS/MS) analysis, and they were highlighted in yellow. (C) The interaction between exogenous USP5 and ILF2 was verified by reciprocal co-immunoprecipitation assays (Co-IPs) with the anti-Myc tag or anti-Flag tag antibody. (D) HCT116 cells were lysed for reciprocal Co-IPs with the anti-USP5 or anti-ILF2 antibody to verify the interaction between endogenous USP5 and ILF2. (E-G) Seven CRC cell lines (E) and five pairs of primary CRC paracancerous and cancerous tissues (F) were lysed for immunoblotting (IB) to determine the protein levels of USP5 and ILF2. GAPDH was used as a loading control. The optical density was also measured, and the correlation analysis was conducted based on the expression levels of ILF2 and USP5 (G).

USP5 was a deubiquitinating enzyme, we then detected whether the ubiquitination of ILF2 was regulated by USP5. As shown in **Figure 4F**, the Co-IP assay showed that overexpression of USP5 obviously inhibited the poly-ubiquitination of ILF2. But knockdown of USP5 enhanced the poly-ubiquitination of ILF2 (**Figure 4G**). These results indicated that the stability of ILF2 protein was upregulated by USP5 via its deubiquitination activity.

ILF2 abolishes the effects of USP5 inhibitor in colorectal cancer cells

Next, CRC cells were incubated with increasing concentrations of WP1130 (a reported USP5 inhibitor), and the results showed that inhibiting USP5 by WP1130 markedly decreased the protein level of ILF2 (**Figure 5A**), but not the mRNA level (**Figure 5B** and **5C**), which further indicated that USP5 affected ILF2 primarily at the protein stability level. The anti-tumor activities of WP1130 in CRC cells were also verified by CCK-8 assay (**Figure 5D**). Then, ILF2 or USP5 was overexpressed in CRC cells, and further studies showed that overexpression of ILF2 or USP5 abolished the anti-tumor activities of WP1130 in CRC cells (**Figure 5E** and **5F**), which further suggested that WP1130's effects on CRC growth were specifically mediated through USP5 inhibition. **Figure 5G** also revealed the schematic model of USP5/ILF2 axis in CRC carcinogenesis.

Discussion

It is known that ILF2 predominantly forms a heterodimer with ILF3 to bind to DNA enhancers,

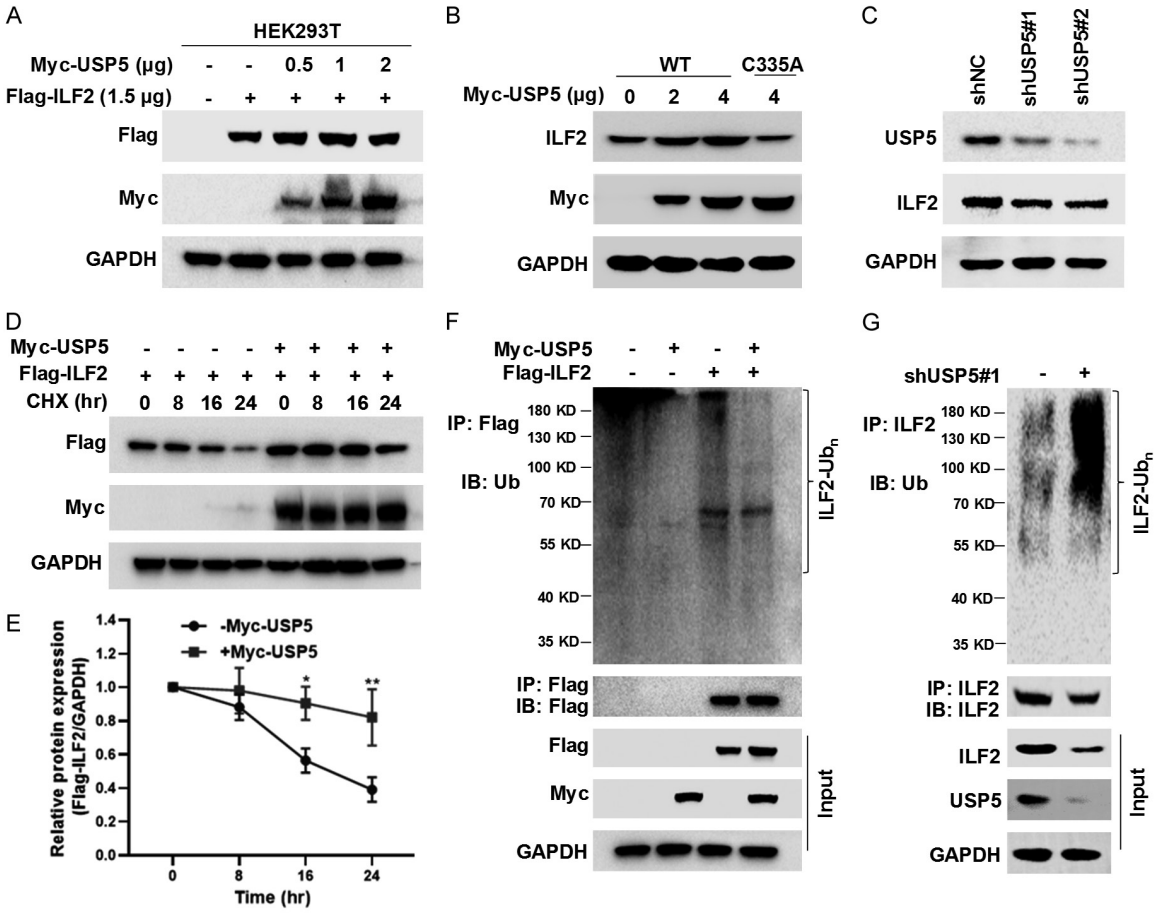

Figure 4. USP5 accumulates ILF2 by reducing the poly-ubiquitination of ILF2. (A) HEK293T cells were transfected with indicated Myc-USP5 and Flag-ILF2 plasmids for 36 hours, followed by immunoblotting (IB) against Flag, Myc and GAPDH. (B) The wild-type (WT) or mutated (C335A) USP5 plasmids with a Myc tag were transfected into HCT116 cells. Thirty-six hours later, transfected cells were lysed for IB against ILF2, Myc and GAPDH. (C) HCT116 cells were infected with indicated shRNA-derived lentivirus for 72 hours, followed by IB against USP5, ILF2 and GAPDH. (D, E) Myc-USP5 and Flag-ILF2 plasmids were transfected into HEK293T cells for 24 hours, and then transfected cells were incubated with 50 μg/ml cycloheximide (CHX) for indicated times. Then, cells were lysed for IB (D) and optical density was measured (E). Data in (E) were the mean ± SD, and analyzed by repeated measures two-way ANOVA followed by Bonferroni's post hoc test. (F) HEK293T cells were transfected with indicated Myc-USP5 or Flag-ILF2 plasmids for 36 hours, and then transfected cells were lysed for co-immunoprecipitation (Co-IP) with the anti-Flag antibody. (G) HCT116 cells infected with shNC or shUSP5#1-derived lentivirus were lysed for Co-IP with an anti-ILF2 antibody. IP, immunoprecipitation. $^{*}P < 0.05$, $^{**}P < 0.01$.

and promotes gene transcription [25]. Recent studies have shown that dysregulation of ILF2 results in serious consequences for the initiation and progression of many diseases, including tumors [25]. Notably, ILF2 was found elevated in CRC, and its upregulation predicted a poor index for CRC patients in this study. Our further investigations showed that knockout of ILF2 inhibited CRC cell growth in vitro, and suppressed tumor growth of CRC in vivo. Given these results, our present study strongly demonstrated that ILF2 was functional in CRC, and exerted tumor-promoting activities. Similarly, ILF2 has also been found to be amplified, and to promote cell proliferation by facilitating cell cycle progression in other tumors [26, 27].

In most events, protein homeostasis is precisely controlled by the ubiquitin-proteasome system (UPS) to ensure the effectiveness of certain proteins in the cells, and protein ubiquitination mediated by UPS is one of the main ways for protein degradation [28-30]. To investigate whether ILF2 was regulated by UPS, a deep learning model Degpred to predict degrons directly from protein sequences was

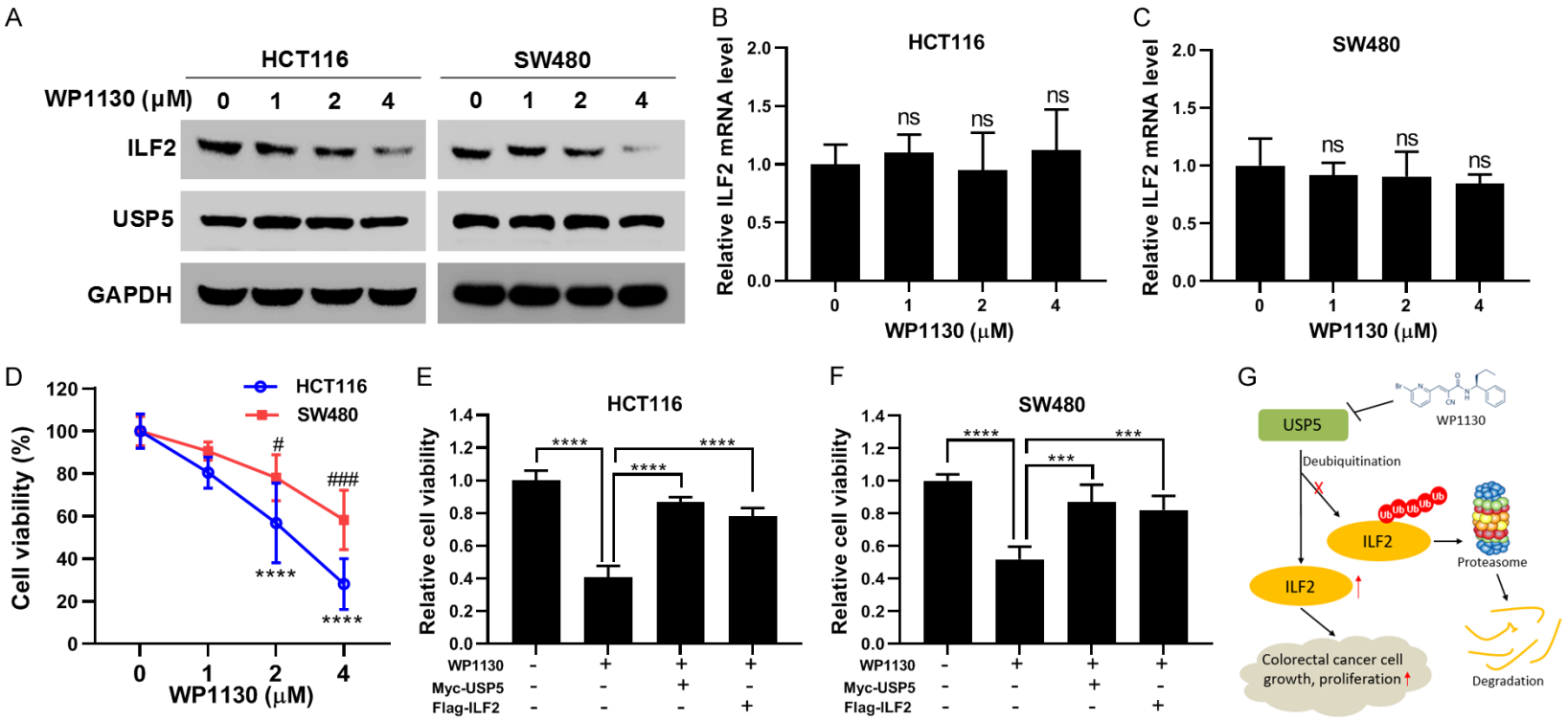

Figure 5. ILF2 upregulation attenuates the effects of WP1130 on colorectal cancer cells. (A-C) HCT116 and SW480 cells were incubated with increasing concentrations of WP1130 overnight, and then cells were lysed for immunoblotting (IB) against ILF2, USP5 and GAPDH (A), or cells were prepared for qRT-PCR analysis to detect the mRNA levels of ILF2 (B, C). Data were analyzed by one-way ANOVA followed by Dunnett's multiple comparisons test. (D) HCT116 and SW480 cells were incubated with increasing concentrations of WP1130 for 24 hours, followed by Cell Counting Kit-8 (CCK-8) assay. Data were the mean ± SD of three independent experiments, and analyzed by two-way ANOVA followed by Tukey's multiple comparisons test. (E, F) HCT116 (E) or SW480 (F) cells transfected with empty vector, Myc-USP5 or Flag-ILF2 plasmids were incubated with 4 μM WP1130 or vehicle for 24 hours, followed by CCK-8 assay. Data were analyzed by one-way ANOVA followed by Tukey's multiple comparisons test. (G) Schematic model indicated the function of USP5/ILF2 axis in CRC carcinogenesis. ns means not significant. $^{***}P < 0.001$, $^{****}P < 0.0001$; $^{\#}P < 0.05$, $^{\#\#\#}P < 0.001$.

used [18]. And the model indicated that there were predicted degrons in the sequence of ILF2 protein, which revealed that ILF2 may be mediated by UPS. Consistently, our results confirmed that ILF2 protein could be accumulated by the proteasome inhibitor MG132, and Co-IP assay also showed that ILF2 was poly-ubiquitinated. A paper published recently also confirmed our results that ILF2 underwent into ubiquitin-mediated proteasomal degradation [31]. Although, it was reported that Cereblon acted as a potential E3 for mediating ubiquitination of ILF2 [31], no one has yet discovered any deubiquitinating enzymes (DUBs) for ILF2 deubiquitination. The ubiquitination of proteins is a dynamic and reversible process, and DUBs can reverse the signals of ubiquitin that most DUBs remove ubiquitin moieties from proteins to prevent substrates from degradation [32]. Interestingly, our previous quantitative proteomics discovered a series of USP5-interacting proteins, and ILF2 was also included [17], which indicated that USP5 may be a DUB that regulated the stability of ILF2 protein. Our further experiments also confirmed that ILF2 bound to USP5, and the protein stability of ILF2 was positively regulated by USP5 in CRC cells. The stability of ILF2 mediated by USP5 may further explain why ILF2 was accumulated and elevated in CRC, which helps us to better understand the mechanism of ILF2 in CRC development. To elucidate the mechanistic link between ILF2 stabilization and downstream oncogenic signalings, we hypothesize that stabilized ILF2 may activate key pathways such as CCND1, c-Myc or NF-κB. Given that knockout of ILF2 was found decrease CCND1 expression in the present study, ILF2 stabilization may enhance the expression of genes involved in cell cycle progression (such as CCND1). While further validation is required, this provides a possible mechanism by which stabilized ILF2 contributes to CRC carcinogenesis.

Our findings in this study have demonstrated that USP5 stabilizes ILF2 in CRC cells. Previous studies have shown that the substrates and mechanisms of USP5 vary considerably in CRC cells, highlighting its functional diversity. For example, USP5 has been shown to deubiquitinate and stabilize TUFM to promote CRC cell growth [17], and to induce metastasis by deubiquitinating Snail [33]. Moreover, USP5 was also reported to suppress ferroptosis by promoting the lysosomal degradation of YBX3 [34]. Our findings in this study further underscores that USP5 exerts its tumor-promoting effects through multiple pathways. In addition, although this study provides the evidences for a USP5-mediated mechanism to regulate the protein stability of ILF2 in CRC cells, further studies are needed on whether there are other DUBs besides USP5. Moreover, our present study does not investigate how USP5 inhibits E3-mediated ILF2 degradation, which will be elucidated in our future work.

Conclusion

In summary, our present study has specified the function of ILF2 in CRC in that ILF2 contributes to CRC cell proliferation. We also demonstrated that the protein stability of ILF2 was enhanced by USP5. Inhibiting USP5 by WP1130 suppressed cell viability of CRC and decreased the expression of ILF2. Our present results suggest that targeting the USP5/ILF2 axis could be a potential therapeutic strategy worthy of further investigation.

Acknowledgements

This study was supported by the Fundamental Research Funds for the Central Universities (No. 22120240280), Open Project of Key Laboratory of Embedded System and Service Computing (Tongji University), Ministry of Education (No. ESSCKF 2024-08), Anhui Provincial Natural Science Foundation (No. 2308085MH280), and Natural Science Research Project of Anhui Educational Committee (2024AH040240).

Disclosure of conflict of interest

None.

Address correspondence to: Yili Yang, China Regional Research Center, International Centre for Genetic Engineering and Biotechnology, 8 Taohongjing Road, Taizhou 225300, Jiangsu, P. R. China. Tel: +86-18702169867; E-mail: nathanyang@icgeb.cn; Peng Yang, Department of Emergency Medicine, The First Affiliated Hospital of Soochow University, 899 Pinghai Road, Suzhou 215006, Jiangsu, P. R. China. Tel: +86-13806131182; E-mail: yangpeng@suda.edu.cn

References

[1] Zhang Y, Gao T, Wu M, Xu Z and Hu H. Value analysis of ITLN1 in the diagnostic and prog-

nostic assessment of colorectal cancer. Transl Cancer Res 2024; 13: 2877-2891.
[2] Morgan E, Arnold M, Gini A, Lorenzoni V, Cabasag CJ, Laversanne M, Vignat J, Ferlay J, Murphy N and Bray F. Global burden of colorectal cancer in 2020 and 2040: incidence and mortality estimates from GLOBOCAN. Gut 2023; 72: 338-344.
[3] Li X, Chen T, Cai Y, Zhang J, Wang Y, Wang J, Mao X, Xu L, Li D, Wang Y and Wang X. CircSETD3 interrupts the bidirectional positive feedback of ErbB3 and Akt by sponging miR-4667-5p to inhibit colorectal cancer progression and cetuximab resistance. Int J Biol Macromol 2025; 318: 145352.
[4] Niekamp P and Kim CH. Microbial metabolite dysbiosis and colorectal cancer. Gut Liver 2023; 17: 190-203.
[5] Zuo S, Huang Y and Zou J. The role of the gut microbiome in modulating immunotherapy efficacy in colorectal cancer. IUBMB Life 2024; 76: 1050-1057.
[6] Wang X, Sun T, Fan J, Zuo X and Mao J. Gastrin-related circRNA_0017065 promotes the proliferation and metastasis of colorectal cancer through the miR-3174/RBFOX2 axis. Biol Direct 2024; 19: 75.
[7] Zhang Y, Li X, Wang C, Zhang M, Yang H and Lv K. lncRNA AK085865 promotes macrophage M2 polarization in CVB3-induced VM by regulating ILF2-ILF3 complex-mediated miRNA-192 biogenesis. Mol Ther Nucleic Acids 2020; 21: 441-451.
[8] Ni T, Mao G, Xue Q, Liu Y, Chen B, Cui X, Lv L, Jia L, Wang Y and Ji L. Upregulated expression of ILF2 in non-small cell lung cancer is associated with tumor cell proliferation and poor prognosis. J Mol Histol 2015; 46: 325-35.
[9] Cheng S, Jiang X, Ding C, Du C, Owusu-Ansah KG, Weng X, Hu W, Peng C, Lv Z, Tong R, Xiao H, Xie H, Zhou L, Wu J and Zheng S. Expression and critical role of interleukin enhancer binding factor 2 in hepatocellular carcinoma. Int J Mol Sci 2016; 17: 1373.
[10] Zhao M, Liu Y, Chang J, Qi J, Liu R, Hou Y, Wang Y, Zhang X, Qiao L and Ren L. ILF2 cooperates with E2F1 to maintain mitochondrial homeostasis and promote small cell lung cancer progression. Cancer Biol Med 2019; 16: 771-783.
[11] Zhang X, Bustos MA, Gross R, Ramos RI, Takeshima TL, Mills GB, Yu Q and Hoon DSB. Interleukin enhancer-binding factor 2 promotes cell proliferation and DNA damage response in metastatic melanoma. Clin Transl Med 2021; 11: e608.
[12] Wan C, Gong C, Ji L, Liu X, Wang Y, Wang L, Shao M, Yang L, Fan S, Xiao Y, Wang X, Li M, Zhou G and Zhang Y. NF45 overexpression is associated with poor prognosis and enhanced cell proliferation of pancreatic ductal adenocarcinoma. Mol Cell Biochem 2015; 410: 25-35.
[13] Wen-Jian Y, Song T, Jun T, Kai-Ying X, Jian-Jun W and Si-Hua W. NF45 promotes esophageal squamous carcinoma cell invasion by increasing Rac1 activity through 14-3-3ε protein. Arch Biochem Biophys 2019; 663: 101-108.
[14] Li J, Wang Y, Luo Y, Liu Y, Yi Y, Li J, Pan Y, Li W, You W, Hu Q, Zhao Z, Zhang Y, Cao Y, Zhang L, Yuan J and Xiao ZJ. USP5-Beclin 1 axis overrides p53-dependent senescence and drives Kras-induced tumorigenicity. Nat Commun 2022; 13: 7799.
[15] Zhang X, Chen T, Li Z, Wan L, Zhou Z, Xu Y, Yan D, Zhao W and Chen H. NORAD exacerbates metabolic dysfunction-associated steatotic liver disease development via the miR-511-3p/Rock2 axis and inhibits ubiquitin-mediated degradation of ROCK2. Metabolism 2025; 164: 156111.
[16] Ning F, Xin H, Liu J, Lv C, Xu X, Wang M, Wang Y, Zhang W and Zhang X. Structure and function of USP5: insight into physiological and pathophysiological roles. Pharmacol Res 2020; 157: 104557.
[17] Xu X, Huang A, Cui X, Han K, Hou X, Wang Q, Cui L and Yang Y. Ubiquitin specific peptidase 5 regulates colorectal cancer cell growth by stabilizing Tu translation elongation factor. Theranostics 2019; 9: 4208-4220.
[18] Hou C, Li Y, Wang M, Wu H and Li T. Systematic prediction of degrons and E3 ubiquitin ligase binding via deep learning. BMC Biol 2022; 20: 162.
[19] Wang C, Huang K, Yang J, Xu Q, Kuai J, Zhang G and Wang X. YTHDF1 promotes pancreatic cancer cell progression by enhancing SF3B2 translation though m6A modification. J Biochem 2025; 177: 425-435.
[20] Li L, Hao S, Gao M, Liu J, Xu X, Huang J, Cheng G and Yang H. HDAC3 inhibition promotes antitumor immunity by enhancing CXCL10-mediated chemotaxis and recruiting of immune cells. Cancer Immunol Res 2023; 11: 657-673.
[21] Zhou B, Fang F, Zhang Y, Li Z, Hu Y, Li Y, Jiao W, Wu Y, Wan X, Yang Y, Zhang F, Xu L, Ji T, Pan J and Hu S. Core transcriptional regulatory circuitry molecule ZNF217 promotes AML cell proliferation by up-regulating MYB. Int J Biol Sci 2025; 21: 1966-1983.
[22] Gu M, Jiang B, Li H, Zhu D, Jiang Y and Xu W. Aldolase A promotes cell proliferation and cisplatin resistance via the EGFR pathway in gastric cancer. Am J Transl Res 2022; 14: 6586-6595.
[23] Liu B, Chen Z, Li Z, Zhao X, Zhang W, Zhang A, Wen L, Wang X, Zhou S and Qian D. Hsp90alpha

promotes chemoresistance in pancreatic cancer by regulating Keap1-Nrf2 axis and inhibiting ferroptosis. Acta Biochim Biophys Sin (Shanghai) 2024; 57: 295-309.
[24] Zhu L, Shen XB, Yuan PC, Shao TL, Wang GD and Liu XP. Arctigenin inhibits proliferation of ER-positive breast cancer cells through cell cycle arrest mediated by GSK3-dependent cyclin D1 degradation. Life Sci 2020; 256: 117983.
[25] Li Y, Wang M, Yang M, Xiao Y, Jian Y, Shi D, Chen X, Ouyang Y, Kong L, Huang X, Bai J, Hu Y, Lin C and Song L. Nicotine-induced ILF2 facilitates nuclear mRNA export of pluripotency factors to promote stemness and chemoresistance in human esophageal cancer. Cancer Res 2021; 81: 3525-3538.
[26] Chiu CL, Li CG, Verschueren E, Wen RM, Zhang D, Gordon CA, Zhao H, Giaccia AJ and Brooks JD. NUSAP1 binds ILF2 to modulate R-loop accumulation and DNA damage in prostate cancer. Int J Mol Sci 2023; 24: 6258.
[27] Sun T, Li X, Zhang Y, Zou B and Zhang Y. ILF2: a multifaceted regulator in malignant tumors and its prospects as a biomarker and therapeutic target. Front Oncol 2024; 14: 1513979.
[28] Xiong Y, Yu C and Zhang Q. Ubiquitin-proteasome system-regulated protein degradation in spermatogenesis. Cells 2022; 11: 1058.
[29] Cao Y, Li Y, Wang L, Zhang L and Jiang L. Evolution and function of ubiquitin-specific proteases (UBPs): insight into seed development roles in plants. Int J Biol Macromol 2022; 221: 796-805.
[30] Du Y, Chu CM, Zhuo D and Ning JZ. The inhibition of TRIM35-mediated TIGAR ubiquitination enhances mitochondrial fusion and alleviates renal ischemia-reperfusion injury. Int J Biol Macromol 2022; 209: 725-736.
[31] Lian Q, Gao Y, Li Q, He X, Jiang X, Pu Z and Xu G. Cereblon promotes the ubiquitination and proteasomal degradation of interleukin enhancer-binding factor 2. Protein J 2020; 39: 411-421.
[32] Han S, Wang R, Zhang Y, Li X, Gan Y, Gao F, Rong P, Wang W and Li W. The role of ubiquitination and deubiquitination in tumor invasion and metastasis. Int J Biol Sci 2022; 18: 2292-2303.
[33] Hong KS, Ryu KJ, Kim H, Kim M, Park SH, Kim T, Yang JW, Hwangbo C, Kim KD, Park YJ and Yoo J. MSK1 promotes colorectal cancer metastasis by increasing Snail protein stability through USP5-mediated Snail deubiquitination. Exp Mol Med 2025; 57: 820-835.
[34] Qiu H, Liu Y, Zhou H, Hu L, Qi W, Ma H, Liu Y, Li L, Yang N, Huang M, Du R, Meng L, Shi F, Wang B, Yu L, Zhang X and Li G. USP5 regulates ferroptosis in colorectal cancer by targeting the YBX3/SLC7A11 axis through lysosomal degradation. Cell Death Dis 2025; 16: 822.

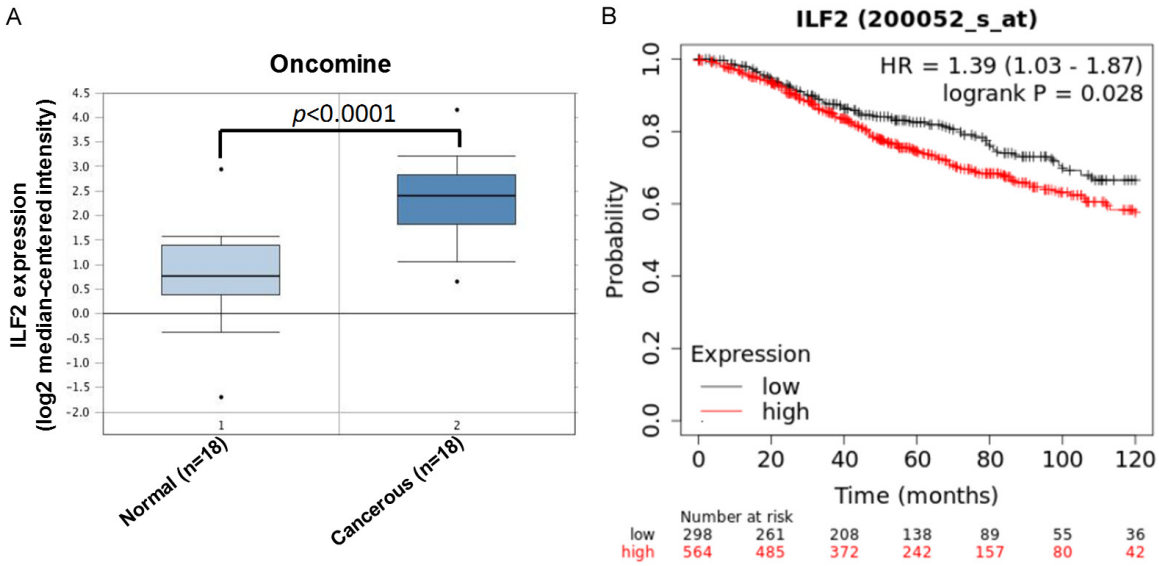

Supplementary Figure 1. ILF2 is upregulated in colon adenocarcinoma and predicted as a negative index for colon cancer patients. A. Oncomine database (https://www.oncomine.org) was used to evaluate the expression of ILF2 in Notterman Colon Statistics. Normal, normal colon tissues (n = 18). Cancerous, colon adenocarcinoma (n = 18). All options were selected as default. Data were analyzed by Student's *t* test. B. Kaplan-Meier Plotter analysis based on colon cancer mRNA database was drawn online (https://kmplot.com) to evaluate the overall survival of colon cancer patients with low or high ILF2. The patients of Stage 1, 2 and 3 were selected. Other options were selected as default.

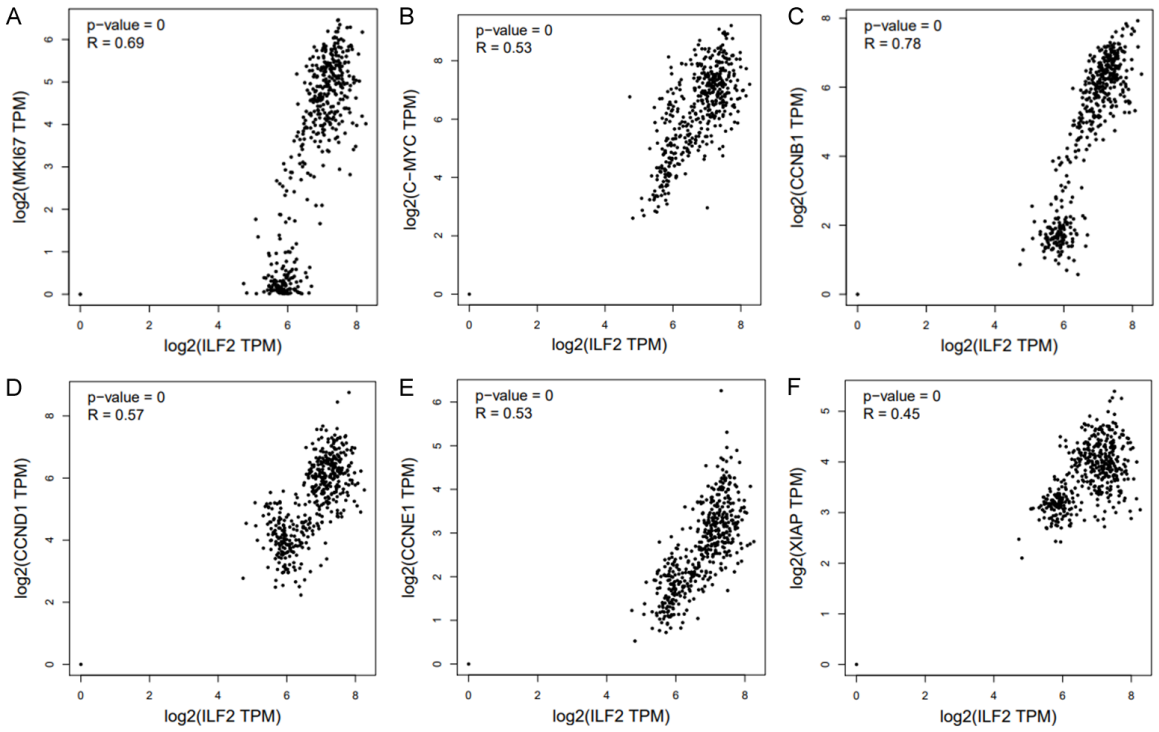

Supplementary Figure 2. The expression of ILF2 is positively correlated with the expression of growth-promoting genes. (A-F) Correlation analyses between ILF2 expression and MKI67 (A), C-MYC (B), CCNB1 (C), CCND1 (D), CCNE1 (E) or XIAP (F) expression in colon adenocarcinoma (COAD) were analyzed by GEPIA database online (http://gepia2.cancer-pku.cn/#correlation). TCGA Tumor, TCGA Normal and GTEx expression datasets were used.

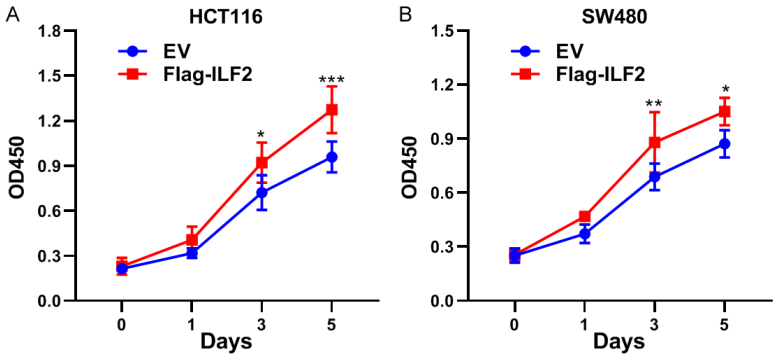

Supplementary Figure 3. Overexpression of ILF2 promotes cell growth of colorectal cancer. (A, B) HCT116 cells (A) or SW480 cells (B) were transfected with the ILF2-overexpressing plasmids Flag-ILF2 or empty vector (EV), and then transfected cells were cultured for indicated time points, followed by CCK-8 assay to assess cell viability. Data were the mean ± SD of three independent experiments, and analyzed by two-way ANOVA followed by Bonferroni's post hoc test. $^{*}P < 0.05$; $^{**}P < 0.01$; $^{***}P < 0.001$.

Protein Information					
Uniport Entry	Q12905	**Entry name**	ILF2_HUMAN	**Gene name**	ILF2 NF45 PRO3063
Function annotation (Click to see function source)		**Short-lived : -**	**Haploinsufficiency : -**	**Oncogene : -**	**Tumor suppressor gene : -**
Known degron			**Known E3s of the protein**	βTrCP2 / PMID: 25515538 βTrCP1/2 / PMID: 25900982	

Predicted degrons and binding E3s (Click here to see FDR of degpred score)					
Degpred region and score	**Degpred sequence**	**Degpred E3**	**ELM region**	**ELM sequence**	**ELM motif**
24-39 (Score : 0.547)	RPFVPHIPFDFYLCEM	-	268-276	YRRCLQILA	DEG_APCC_DBOX_1
380-383 (Score : 0.367)	GEEE	-	1-4	MRGD	DEG_Nend_UBRbox_1
			64-77	LAPNSAEQASILSL	DEG_ODPH_VHL_1

Supplementary Figure 4. Information for the predicted degrons of human ILF2 protein. The degrons of human of ILF2 protein was predicted by Degpred online (http://degron.phasep.pro/detail/Q12905/). All options were selected as default.